



# Study of two G-protein coupled receptor variants of human trace amine-associated receptor 5

Xiaoqiang Wang<sup>1,2</sup>, Karolina Corin<sup>1</sup>, Cyrus Rich<sup>1</sup> & Shuguang Zhang<sup>1</sup>

<sup>1</sup>Center for Biomedical Engineering NE47-379, Massachusetts Institute of Technology, 77 Massachusetts Avenue, Cambridge, MA 02139-4307, USA, <sup>2</sup>Center for Bioengineering and Biotechnology, China University of Petroleum (East China), Qingdao, Shandong 266555, China.

SUBJECT AREAS:  
BIOLOGICAL SCIENCES  
BIOCHEMISTRY  
BIOTECHNOLOGY  
MOLECULAR BIOLOGY

Received  
19 April 2011

Accepted  
18 July 2011

Published  
27 September 2011

Correspondence and  
requests for materials  
should be addressed to  
S.Z. (shuguang@mit.  
edu)

Here we report the study of two bioengineered variants of human trace amine-associated receptor 5 (hTAAR5) that were expressed in stable tetracycline-inducible HEK293S cell lines. A systematic detergent screen showed that fos-choline-14 was the optimal detergent to solubilize and subsequently purify the receptors. Milligram quantities of both hTAAR5 variants were purified to near homogeneity using immunoaffinity chromatography followed by gel filtration. Circular dichroism showed that the purified receptors had helical secondary structures, indicating that they were properly folded. The purified receptors are not only suitable for functional analyses, but also for subsequent crystallization trials. To our knowledge, this is the first mammalian TAAR that has been heterologously expressed and purified. Our study will likely stimulate in the development of therapeutic drug targets for TAAR-associated diseases, as well as fabrication of TAAR-based sensing devices.

**B**iogenic amines are a collection of endogenous functional compounds with an amine group. Classical biogenic amines, such as serotonin, histamine and catecholamines, play important roles as hormones and neurotransmitters in the central and peripheral nervous systems<sup>1-4</sup>. Trace amines are a second class of biogenic amines that are related to classical biogenic amines. These include tyramine, tryptamine, phenylethylamine and octopamine, and are only present in trace amounts in the mammalian nervous system.

Trace amines have long been hypothesized to act as neurotransmitters or neuromodulators like classical biogenic amines. Indeed, disruptive regulation of trace amines is tightly linked to various human disorders including depression, migraine headaches and schizophrenia<sup>4-6</sup>. However, a full picture of how trace amines function *in vivo*, and how their dysregulation causes such diseases, has not been revealed despite several decades of efforts. The relatively recent discovery of trace amine-associated receptors (TAARs) finally opened the door towards understanding the molecular and physiological roles of these molecules<sup>7-9</sup>.

TAARs comprise a structurally and functionally distinct subfamily of G-protein coupled receptors (GPCRs)<sup>1</sup>. The family includes members that are highly specific for trace amines, as well as members that do not respond to trace amines at all, suggesting other potential roles for TAARs. Indeed, TAAR mRNA transcripts have been found in several locations, including the kidneys, skeletal muscle, leukocytes, mouse olfactory epithelium, and the amygdala, a deep tissue inside the brain which is associated with the sense of smell<sup>2,9-11</sup>. Interestingly, at least 3 TAAR members found in the mouse olfactory epithelium recognized volatile amines present in urine. This suggests that TAARs may serve a chemosensory function in addition to what was previously thought, and may form a family of receptors in the mouse olfactory epithelium distinct from olfactory receptors<sup>2</sup>. Moreover, the similarity in function with olfactory receptors, which have the ability to recognize and discriminate between myriad volatile molecules on the order of parts per million or billion<sup>12</sup> indicates that TAARs may be equally sensitive, and could potentially be exploited for use in biologically-based sensors.

The human trace amine-associated receptor 5 (hTAAR5) is one of 6 human TAARs identified to date. Known previously as putative neurotransmitter receptor (PNR), hTAAR5 shows significant sequence homology to human neurotransmitter receptors, and is probably the first mammalian TAAR discovered<sup>7,11</sup>. Furthermore, hTAAR5 mRNA has been found in several tissues, including skeletal muscle, kidney, and the amygdala<sup>9,11</sup>. Study of the structure and function of hTAAR5 is thus likely to yield insights into the physiological importance of this relatively novel GPCR subfamily.



Detailed structural knowledge of TAARs is necessary in order to understand how they function at the molecular level, as well as to design therapies and sensors<sup>13</sup>. A major obstacle towards structural and functional studies of TAARs and other membrane proteins is the notorious difficulty of easily and affordably obtaining milligram quantities<sup>14,15</sup>. Here we report the expression and purification of two synthetic variants of hTAAR5 in stable tetracycline-inducible HEK293S cell lines<sup>16–18</sup>. One variant was the native receptor, while the second was fused to T4-Lysozyme to increase the potential for crystal growth. Both variants were engineered to facilitate detection and purification. Milligram quantities of both variants could be produced at high purity. Circular dichroism showed that both purified hTAAR5 receptors had alpha-helical secondary structures. This suggests that the receptors were properly folded, and are suitable for structural and functional studies. To our knowledge, this is the first mammalian TAAR that has been heterologously expressed and purified. Our study will likely further stimulate to the development of TAAR as therapeutic drug targets, as well as fabrication of TAAR-based sensing devices.

## Results

**General considerations in the design of two hTAAR5 variants.** The native human trace amine-associate receptor 5 (hTAAR5) was used as a template for two hTAAR5 variants. The first variant was designated as “hTAAR5”. To simplify protein detection and purification, the *Strep*-tag II (WSHPQFEK) was added to the N-terminus and the rho1D4 epitope tag (TETSQVAPA) was added to the C-terminus<sup>16–18</sup>. To increase protein homogeneity, the consensus N-glycosylation site was removed by replacing asparagine at position 21 with glutamine (N21Q). The second variant was designated as “hTAAR5-T4L”. It had the same sequence as the first variant with residues 2–161 of T4 phage lysozyme inserted after residue Lys266. This insertion is predicted to be at the end of the third intracellular loop<sup>19,20</sup>, and was done to further facilitate the growth of high quality crystals. The expression of these hTAAR5 variants in HEK293S cells was compared, as well as their solubilization and purification from these cells. The secondary structures of the purified receptors were likewise compared.

**Construction and selection of stable hTAAR5 and hTAAR5-T4L-inducible HEK293S cell lines.** To minimize the toxic effects of receptor overexpression, stable hTAAR5 and hTAAR5-T4L-inducible HEK293S cell lines were created using the Invitrogen T-REx tetracycline regulation system<sup>16–18</sup>. These cells can be grown to the ideal density, and receptor production can be induced by the addition of tetracycline. Up to 60 cell clones were screened for hTAAR5 or hTAAR5-T4L expression. Each clone was induced for 48 hours under three parallel expression conditions: 1) in plain media (–), 2) in media supplemented with 1 μg/ml tetracycline (+), and 3) in media supplemented with tetracycline and 2.5 mM sodium butyrate enhancer (++). A dot blot analysis with a monoclonal antibody against the rho-tag was performed to analyze the receptor expression level of each clone under each condition. Results for the expression of hTAAR5 and hTAAR5-T4L from the first 15 clones screened are shown in Figures 1a and 1b. The dot blot shows that clones have different expression levels under identical induction conditions. For hTAAR5, clone 2 and clone 8 had the highest level of expression after 48h induction in media supplemented with 1 μg/ml tetracycline and 2.5 mM sodium butyrate enhancer, but maintained undetectable background levels in the absence of tetracycline. For hTAAR5-T4L, clone 5 and clone 8 showed high-level expression but maintained undetectable background levels without induction.

Western blots against the rho1D4 tag were employed to further analyze hTAAR5 expression from clone 2 and clone 8, as well as hTAAR5-T4L expression from clone 5 and clone 8 (Figure 1c). The blots revealed one major immunoreactive band from the hTAAR5 samples at approximately 33 kDa. In contrast, the hTAAR5-T4L samples had three major bands at approximately 47 kDa, 100 kDa and 15 kDa. The former two bands correspond in size to monomeric and dimeric forms of hTAAR5-T4L. The third 15 kDa immunoreactive band is postulated to originate from enzymatic digestion of the recombinant protein. Both blots showed that clone 8 from hTAAR5 and hTAAR5-T4L had the highest expression levels. These clones were thus selected for all subsequent experiments.

The expression of hTAAR5 and hTAAR5-T4L was further optimized by varying the concentrations of both tetracycline and sodium butyrate (Figure 2). Varying the concentration of either tetracycline

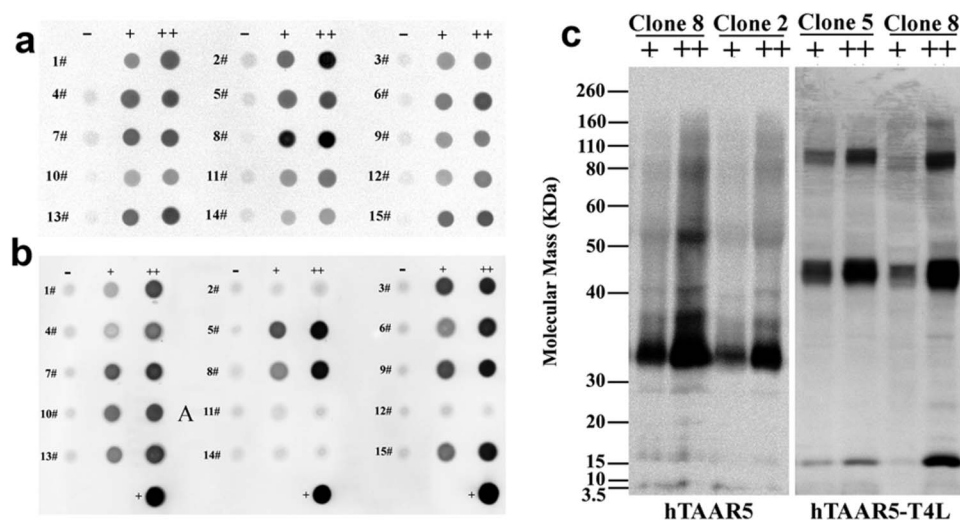


**Figure 1 | Construction of stable hTAAR5 and hTAAR5-T4L-inducible HEK293S cell lines using the T-REx system (Invitrogen).** Dot blot analysis was used to analyze the hTAAR5 (a) or hTAAR5-T4L (b) expression level of different clones after selective incubation. The numbers identify each. Three 48-hour induction conditions were tested in parallel for each clone: 1) in plain media (–), 2) in media supplemented with 1 μg/ml tetracycline (+), or 3) in media supplemented with 1 μg/ml tetracycline plus 2.5 mM sodium butyrate (++). The three dots at the bottom of b are positive controls. (c) Western blot analysis using an anti-rho-tag monoclonal antibody was also used to further analyze the expression level of hTAAR5 from clones 2 and 8, or the expression level of hTAAR5-T4L from clones 5 and 8. The symbols “+” and “++” represent the same induction conditions as those in the dot blot analysis.



or sodium butyrate affected hTAAR5-T4L expression, with the latter showing a more significant effect (Figure 2). As the concentration of sodium butyrate is increased from 0mM to 2.5mM under a constant tetracycline concentration, receptor expression also increases. However, when the concentration of sodium butyrate is increased from 2.5mM to 5mM, expression of hTAAR5-T4L drops, presumably due to the toxic effect of receptor overexpression. The influence of tetracycline and sodium butyrate on hTAAR5 expression showed a similar trend. For subsequent experiments, the hTAAR5 and hTAAR5-T4L clones were treated with 2.5mM sodium butyrate and 1 $\mu$ g/ml tetracycline for 48h.

**Detergent screening of hTAAR5 and hTAAR5-T4L for solubilization from HEK293S cells.** Selection of a suitable detergent is crucial in order to solubilize membrane proteins from the host cell membrane, stabilize them during purification process, and to maximize the final protein yield. However, our understanding of the interaction between detergents and membrane proteins is still limited, and the optimal detergent must be empirically determined. We thus carried out a systematic detergent screen that included representatives from non-ionic, anionic, cationic and zwitter-ionic detergent classes, as well as some detergent mixtures proven effective for solubilizing other GPCRs.

Figure 3 shows the detergent screening results obtained by means of immunoblot analysis. The most effective detergents for solubilizing hTAAR5 were n-Dodecyl- $\beta$ -iminodipropionic acid (monosodium salt), the fos-choline series, and n-Tetradecyl-N,N-dimethylamine-N-oxide (TDAO) (Figure 3a). Interestingly, the most effective detergents for solubilizing hTAAR5-T4L were slightly different (Figure 3b), and included sodium dodecanoyl sarcosine instead of n-Tetradecyl-N,N-dimethylamine-N-oxide (TDAO). This difference is most likely due to the structural variation between hTAAR5 and hTAAR5-T4L. The ability of the fos-choline series to solubilize both receptor variants is not surprising, as they are structurally related to phosphatidylcholine, a phospholipid and major constituent of the lipid bilayer of mammalian cells. Because of this, and because previous studies have shown that the fos-choline series, and especially fos-choline 14 (FC-14), are effective for stabilizing GPCRs<sup>17,18,21</sup>, FC-14 was used for all subsequent experiments.

**Purification of heterologously expressed hTAAR5 and hTAAR5-T4L.** A two-step purification method was used to purify hTAAR5 and hTAAR5-T4L<sup>16–18</sup>. First, CNBr-activated Sepharose 4B beads linked to the mouse monoclonal rho1D4 antibody were used to capture detergent solubilized receptors. Following a thorough wash procedure to remove non-specific impurities, the captured receptors

were eluted by the addition of an excess of rho1D4 elution peptide (TETSQVAPA). Fractions were subjected to SDS-PAGE followed by Western blot analysis. Figure 4 shows the Western blots of immunoaffinity-purified hTAAR5-T4L. No hTAAR5-T4L was detected in the flow through, indicating that the receptor was completely captured by the beads. The captured hTAAR5-T4L was eluted primarily in the first 3 fractions. Similar results were obtained for hTAAR5.

To further purify the receptor and to remove the elution peptide, the eluted receptor fractions were concentrated and then subjected to gel filtration on an Äkta FPLC system. Column flowthrough was monitored by UV absorption at 280nm, 254nm and 215nm, and was separated into fractions by an auto-fraction collector. Figure 5a shows the gel filtration chromatogram of hTAAR5-T4L from ~9g of induced HEK293S cells. Seven distinct peaks were observed. The peak fractions were pooled, concentrated, and assayed on a Western blot or total protein stain. Figures 5b and 5c show the Western blot and total protein stain results. Peak 4 contained monomeric hTAAR5-T4L (>90% purity) while earlier peaks primarily contained dimeric (peak 3) and aggregated/oligomerized (peak 2) forms. Peak 1 contained no components detectable by either Western blotting or by total protein staining. Peaks 5 and 6 mainly contained truncated forms of hTAAR5-T4L, which were present prior to purification (Figure 1c). Peak 7 contained the rho1D4 elution peptide. The final yield of purified hTAAR5-T4L monomer was ~1.5 milligrams. Mass spectrometry analysis using samples isolated from SDS-PAGE gel bands confirmed that the identity of the monomer and dimer protein bands was hTAAR5-T4L. Similar results were seen for hTAAR5. Figure 5d–5f shows the gel filtration results for hTAAR5 purified from ~5g of induced HEK293S cells. Six distinct peaks can be seen (Figure 5d). A western blot (Figure 5e) and total protein stain (Figure 5f) showed that peak 3 contained monomeric hTAAR5 at >90% purity. The final yield of purified hTAAR5 monomer was >1 milligram. Mass spectrometry analysis confirmed that the identity of the 33kDa band was hTAAR5. These results show that a two-step purification method can be used to obtain milligram quantities of high quality hTAAR5 and hTAAR5-T4L.

**Secondary structure analysis of purified hTAAR5 and hTAAR5-T4L.** Circular dichroism (CD) was used to analyze the secondary structures of purified hTAAR5 and hTAAR5-T4L. High-resolution structures of GPCRs show that they have an  $\alpha$ -helical structure<sup>13</sup>. As a member of this family, both variants would be expected to have helical secondary structures. Indeed, transmembrane domain calculations predict that the native hTAAR5 secondary structure is >50%  $\alpha$ -helix (www.uniprot.org/uniprot/O14804). Far-UV CD

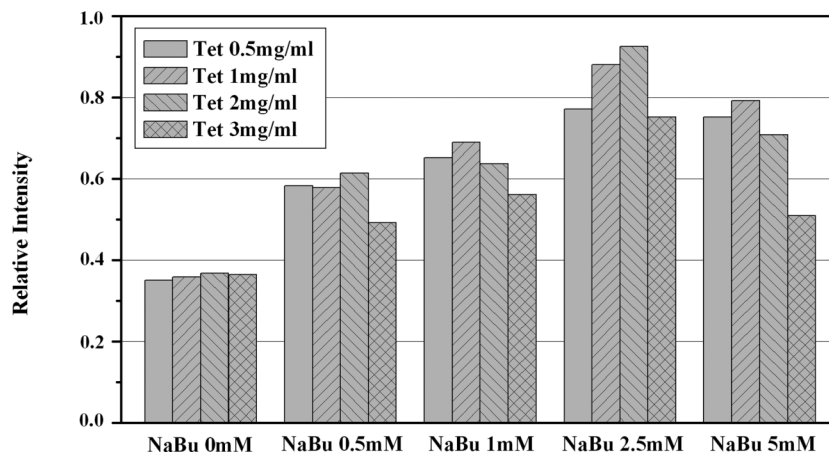


**Figure 2 | Optimization of hTAAR5-T4L expression.** hTAAR5-T4L expression was induced with varying the concentrations of both tetracycline and sodium butyrate. After induction, the samples were harvested and analyzed on a dot blot. The results were quantified by spot densitometry and normalized to the range of 0.0 to 1.0 for ease of comparison.

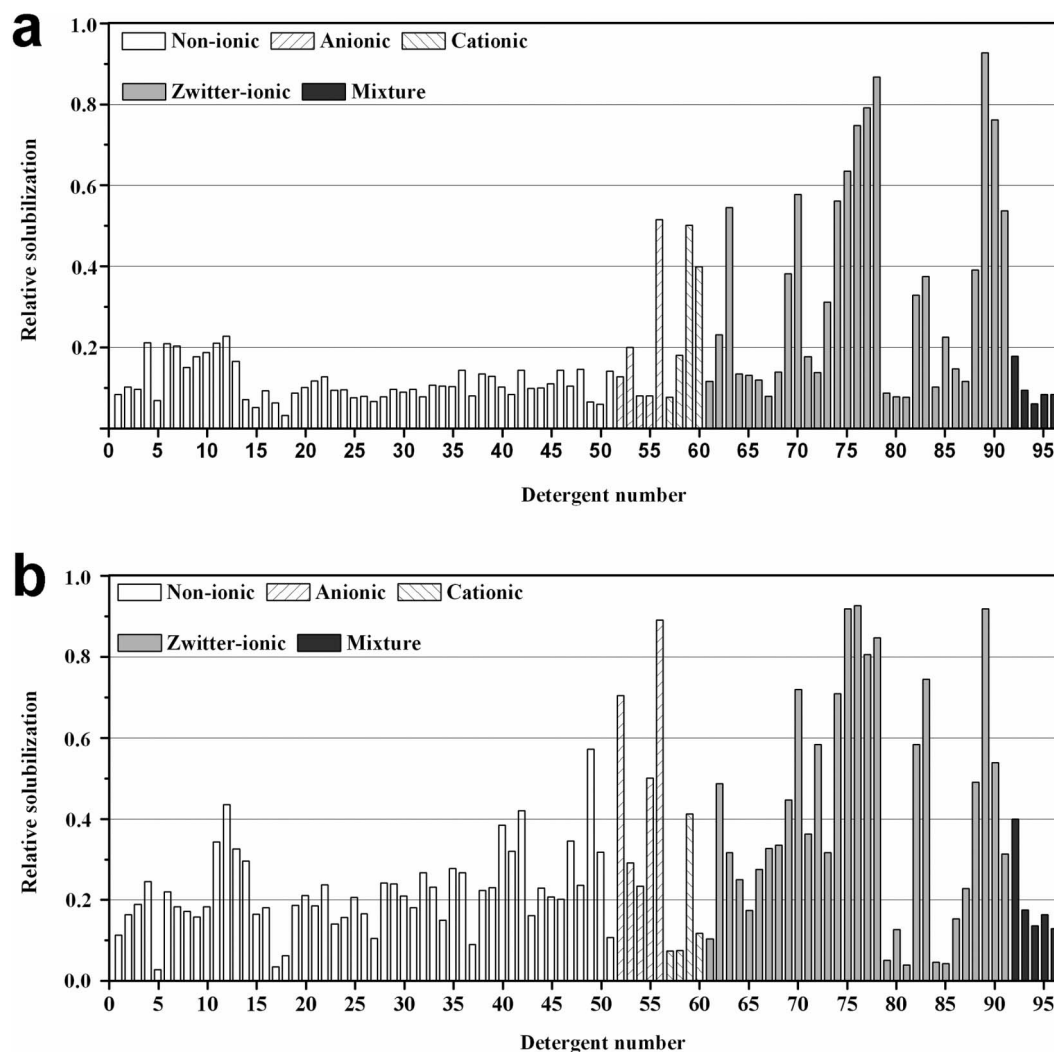


**Figure 3 | Detergent screening for optimal solubilization of hTAAR5 (a) and hTAAR5-T4L (b) expressed in HEK293S cells.** Expression of hTAAR5 or hTAAR5-T4L was induced with tetracycline (1  $\mu$ g/ml) and sodium butyrate (2.5 mM) for 48 h, and receptors were solubilized in PBS containing detergents for 1 hour at 4 °C. In total, 96 detergents or detergent-mixtures were screened. Each integer from 1 to 96 along the x-axis represents a detergent or detergent mixture (see Supplementary Table S1 online for more information about each detergent or detergent mixture). The ability of each detergent or mixtures to solubilize hTAAR5 or hTAAR5-T4L was quantified by spot densitometry and normalized to the range from 0.0 to 1.0 for ease of comparison.

spectroscopy confirmed that the monomeric forms of hTAAR5 and hTAAR5-T4L are predominantly  $\alpha$ -helical (Figure 6). The spectra were analyzed using the K2D2 algorithm which predicted an  $\alpha$ -helix content of  $\sim$ 63% for hTAAR5 and  $\sim$ 69% for hTAAR5-T4L. This difference is presumably due to the insertion of T4 lysozyme, which has  $\sim$ 60%  $\alpha$ -helical content<sup>22</sup>. These results indicate that both hTAAR5 variants are folded correctly, even after purification. They further suggest that the receptors are suitable for subsequent crystallization trials and functional analyses.

## Discussion

Evidence suggests that TAARs may have important neurological or olfactory functions. However, although they were discovered a decade ago, great efforts are still required to characterize their structure and function<sup>7</sup>. The primary obstacle in this research has been the difficulty of obtaining sufficient receptor quantities. In this study, we successfully constructed inducible mammalian cell lines and obtained milligram quantities of two hTAAR5 variants by following the method utilized for large-scale production of hOR17-4<sup>16–18</sup>. To our knowledge, this is the first mammalian TAAR that has been heterologously expressed and purified in milligram quantities.

Because the ultimate goal is to determine the TAAR structure, the two hTAAR5 variants were bioengineered to facilitate crystallization. A separate study on the GPCR hOR17-4 showed that glycosylation resulted in two distinct monomer forms of the protein<sup>17,18</sup>. Because TAARs share this site, and because sample inhomogeneity can inhibit crystal growth, the consensus N-glycosylation site for GPCRs was removed through mutation. Western blots of these mutated receptors detected only one monomer form of hTAAR5 or hTAAR5-T4L, suggesting that the samples were homogeneous. Furthermore, because membrane protein crystals primarily form through contacts of soluble domains, phage T4 lysozyme was inserted at the end of the third intracellular loop of the hTAAR5-T4L variant. It is hypothesized that this insertion will facilitate hTAAR5 crystallization by increasing the area of the soluble domain, and hence the potential number of lattice-forming contacts. Indeed, the feasibility of using this method for GPCR structural studies has been demonstrated with the human  $\beta$ 2-adrenergic receptor-T4 lysozyme fusion protein<sup>19, 20</sup>.

We observed that the apparent molecular weights of hTAAR5 or hTAAR5-T4L are smaller than their theoretical values of 40.7 kDa and 58.8 kDa, respectively. This is not uncommon for membrane proteins on gel electrophoresis. Unlike soluble proteins, which are

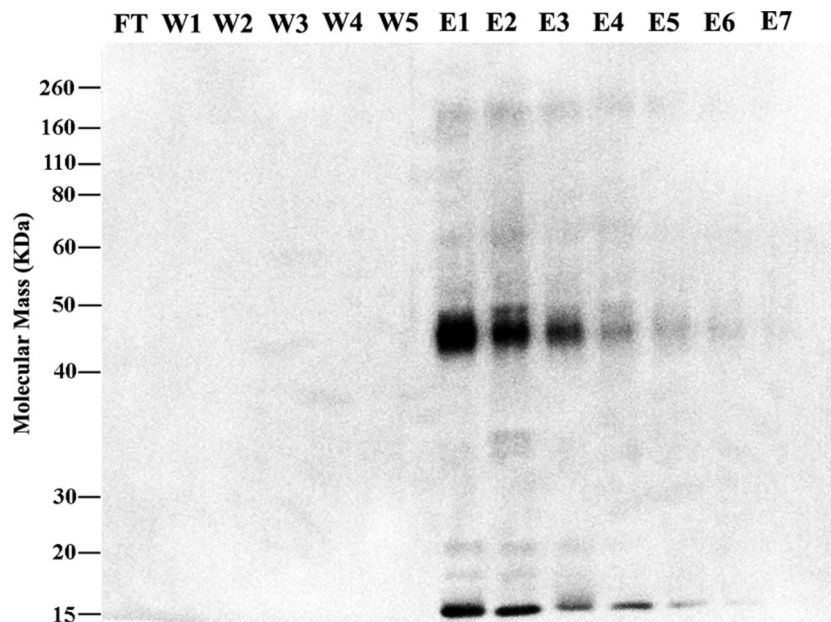


**Figure 4 | Immunoaffinity purification of hTAAR5-T4L.** Induced HEK293S cells were harvested and solubilized. The expressed protein was captured by sepharose beads linked to the anti-rho-tag monoclonal antibody. The captured proteins were washed and then eluted using the rho-tag elution peptide TETSQVAPA. Samples were analyzed on a western blot. Abbreviations: FT, flow through; W, wash; E, elution.

usually boiled before loaded in SDS-PAGE gel, membrane proteins must not be boiled before sample loading since boiling will cause protein aggregation. Since membrane proteins are tightly surrounded by detergent, SDS (also a detergent) alone cannot fully denature membrane proteins in the present other detergent. They thus have a more compact shape, and tend to migrate faster, typically at ~70–85% of their theoretical molecular weight<sup>23</sup>. The coexistence of monomeric and dimeric forms of hTAAR5-T4L has been observed with many other GPCRs<sup>16–18,21,24–26</sup>. Since some studies have shown that the monomeric form is sufficient to activate a G-protein and bind arrestin, further studies are required to understand the function of dimerization and to elucidate its biological significance<sup>27</sup>.

To minimize the toxic effects of receptor overexpression, stable hTAAR5 and hTAAR5-T4L-inducible HEK293S cell lines were constructed. The HEK293S cells can be grown to the ideal density, and receptor production can be induced by the addition of tetracycline at the desired time. Sodium butyrate can be used to enhance expression<sup>16–18</sup>. This approach largely eliminated “leaky expression”, as no background expression of hTAAR5 and hTAAR5-T4L was detectable. This also resulted in more uniform protein samples, as constitutive expression can result in structural or functional inhomogeneity.

It is critical to find a detergent that can purify proteins, stabilize them, and maximize the final protein yield. A systematic detergent screen determined that FC-14 could optimally solubilize hTAAR5 and hTAAR5-T4L from HEK293S cells, and subsequently purify them. Interestingly, this detergent has effectively solubilized other diverse GPCRs<sup>17,18,21</sup>. It should be noted that only 2 of the top 3 detergents for solubilizing hTAAR5 were the same as the top 3 for solubilizing hTAAR5-T4L. This is likely due to structural variations between hTAAR5 and hTAAR5-T4L. More studies of the interactions between detergents and membrane proteins are required to explain this subtle difference.

Although mammalian TAARs were reported as a novel GPCR subfamily in 2001, this is the first time, to our knowledge, that a mammalian TAAR has been heterologously expressed and purified. A two-step purification method was employed to purify hTAAR5 and hTAAR5-T4L to high homogeneity and purity (>90%). About 1mg of hTAAR5 monomer could be purified from 5g of induced

HEK293S cells, and ~1.5mg hTAAR5-T4L monomer could be purified from 9g of cells. Secondary structure analysis using circular dichroism indicated that the purified receptors were correctly folded.

Here we show that a mammalian TAAR can be designed and placed into an inducible mammalian expression system. The resulting full-length protein can be purified to near homogeneity using a two-step purification process. This work represents a significant step towards achieving milligram-scale production of hTAAR for structural and functional studies. The expressed receptors are also suitable for functional studies because the mammalian cell environment is closest to that of tissues in which GPCRs naturally occur. Particularly, mammalian cells can provide a system for studying G-protein interactions with the expressed proteins, as well as downstream signal transduction<sup>28</sup>. Our study may contribute to the development of therapeutic targets, as well as fabrication of TAAR-based bionic sensing devices.

## Methods

**Design of two hTAAR5 variants.** The 337 amino acid sequence of hTAAR5 (accession number NP\_003958.2) was obtained from the NCBI online database. To adapt the hTAAR5 gene for expression in mammalian cells, purification, and structural studies, the following sequence modifications were made: 1) human codon optimization; 2) addition of an N-terminal Strep-tag II (WSHPQFEK) followed by a GSSG linker to facilitate detection and purification; 3) addition of a C-terminal rho1D4 epitope tag (TETSQVAPA) preceded by a GG linker to facilitate detection and purification; 4) alteration of the consensus N-glycosylation sequence (-Asn-Gly-Ser-) by changing the asparagine at position 21 to glutamine (N21Q) to increase the structural homogeneity of target protein; 5) addition of a Kozak consensus sequence (GCCACCACC) immediately 5' to the start codon; 6) addition of an *EcoRI* restriction site at the 5' end and an *XhoI* restriction site at the 3' end of the gene to enable cloning into expression vectors. The hTAAR5 gene with such modifications was designated “hTAAR5”. In addition, a fusion protein termed “hTAAR5-T4L” was also engineered on the structural basis of “hTAAR5” to facilitate protein crystal growth. This protein had residues 2–161 of T4 phage lysozyme inserted after residue Lys266, which is predicted to be at the end of the third intracellular loop. The transmembrane domain prediction of hTAAR5 was performed by the TMHMM Server v.2.0 (<http://www.cbs.dtu.dk/services/TMHMM/>). The two genes were commercially synthesized and subcloned into the T-REx pcDNA4/To inducible expression plasmid (Invitrogen, Carlsbad, CA) by GENEART. The final constructs were verified by DNA sequencing and were used for all subsequent studies.

**Construction of stable inducible cell lines.** The stable hTAAR5- and hTAAR5-T4L-inducible HEK293S cell lines were constructed as previously described<sup>16–18</sup>. Briefly, HEK293S cells stably expressing pcDNA6/Tr (Invitrogen) were cultured in regular

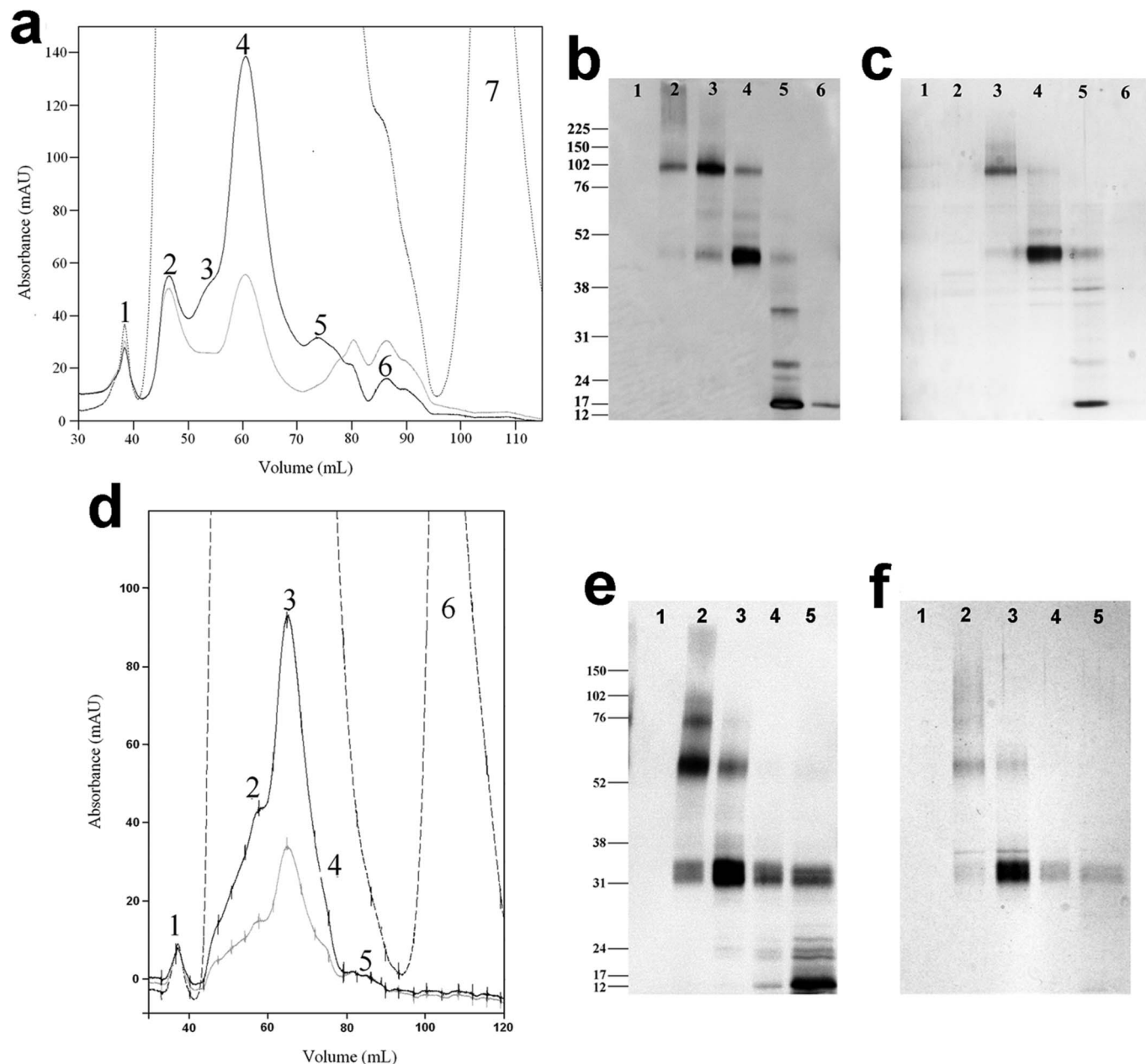


**Figure 5 | Gel filtration purification of hTAAR5-T4L.** (a) Gel filtration of immunoaffinity-purified hTAAR5-T4L from ~9g cells (wet weight). Absorbance was recorded at 280nm (black line), 254nm (gray line), and 215nm (dashed line). Peaks 1-6 (indicated by numbers) were pooled and concentrated. Peak 7 contained the rho1D4 elution peptide TETSQVAPA from the immunoaffinity purification. Both Western blotting (b) and silver staining (c) were employed to analyze the peak fractions. Peak numbers refer to those designated in (a). (d) Gel filtration of immunoaffinity-purified hTAAR5 from ~5g cells (wet weight). Peaks 1–5 (indicated by numbers) were pooled and concentrated. Peak 6 contained the rho1D4 elution peptide TETSQVAPA from the immunoaffinity purification. (e) A Western blot and (f) silver stain were used to analyze the peak fractions.

medium to form monolayers at 37°C and 5% CO<sub>2</sub>. pcDNA4/To plasmids containing the optimized hTAAR5 or hTAAR5-T4L genes were then transfected into these cells using Lipofectamine 2000. After 48 hours, the cells were subjected to drug selection in 5µg/ml blasticidin and 50µg/ml zeocin for 2–3 weeks. The zeocin concentration was then reduced to 25µg/ml. Sixty clones were selected, expanded and screened for inducible expression of hTAAR5 and hTAAR5-T4L. Forty-eight hour expression was induced in each clone under 3 parallel conditions: 1) in plain media (-), 2) media supplemented with 1µg/ml tetracycline (+), or 3) media supplemented with 1µg/ml tetracycline and 2.5mM sodium butyrate enhancer (++). Expression was assayed via dot blots and Western blots. Clones showing the highest inducible expression levels of hTAAR5 and hTAAR5-T4L, while maintaining undetectable expression without induction, were selected and expanded for use in all subsequent experiments.

**Optimization of hTAAR5/hTAAR5-T4L expression.** After stable inducible cell lines were constructed, hTAAR5 and hTAAR5-T4L expression was further optimized by varying the concentrations of tetracycline (inducer) and sodium butyrate (enhancer). For such experiments, hTAAR5 and hTAAR5-T4L inducible cells were

grown to 80–90% confluency at 37°C in 12-well tissue culture plates. They were treated as indicated and then harvested into ice-cold PBS containing Complete Protease Inhibitor Cocktail (Roche, Basel, CH). The receptors were then solubilized by resuspending the cell pellets in 150µl solubilization buffer (PBS + Complete Protease Inhibitor Cocktail + 2% wt/vol FC-14) and rotating them for 1hour at 4°C. The non-solubilized fraction was pelleted by centrifugation at 13,000rpm for 30 minutes. The supernatant was then removed and analyzed by a dot blot. The results were quantified by spot densitometry and normalized to the range of 0.0 to 1.0 for ease of comparison.

**Systematic detergent screening.** In total, 96 detergents or detergent mixtures were screened here. Eighty-eight detergents were chosen from the Solution Master Detergent Kit (Anatrace). Additionally, HEGA-10, NP-40, Digitonin and five detergent mixtures were also chosen because of their effectiveness in solubilizing other GPCRs<sup>29</sup>. Information about each detergent or detergent mixture is provided in Supplementary Table S1 online. The detergent screening process has been described before<sup>16,18,21</sup>.

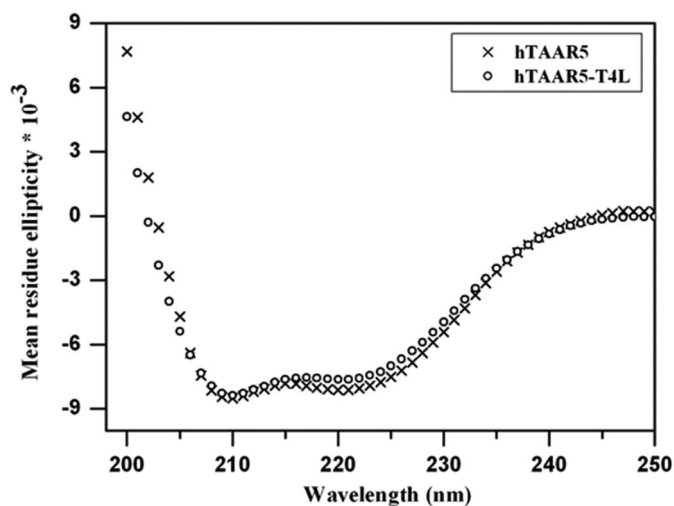


**Figure 6 | Circular dichroism spectra of purified hTAAR5 and hTAAR5-T4L monomers.** Mean residue ellipticity  $[\theta]$  has units of degree  $\times$  cm<sup>2</sup>  $\times$  dmol<sup>-1</sup>. Each spectrum shown is the average of 3 replicate scans. The spectra show typical  $\alpha$ -helical profiles with minima at 208nm and 222nm. The helical contents for hTAAR5 and hTAAR5-T4L are  $\sim$ 63% and  $\sim$ 69%, respectively. These results suggest that hTAAR5 and hTAAR5-T4L are folded correctly.

**Western blot, dot blot and total protein staining analyses.** For Western blotting, protein samples were prepared and loaded in Novex 10% Bis-Tris SDS-PAGE gel (Invitrogen) according to manufacturer's protocol, with the exception that the samples were incubated at room temperature prior to loading as boiling caused membrane protein aggregation. The Full Range Rainbow (GE Healthcare, Waukesha, WI) molecular weight marker was loaded as the protein size standard. After the samples were resolved on an SDS-PAGE gel, they were transferred to a 0.45 $\mu$ m nitrocellulose membrane, blocked in milk (5% non-fat dried milk in TBST) for 1 hour, and incubated with an anti-rho-tag monoclonal antibody (1 : 3000, 1 hour, room temperature). The target proteins were then detected with a goat anti-mouse HRP-conjugated secondary antibody (Pierce, Rockford, IL) (1 : 5000, 1 hour, room temperature) and visualized using the ECL-Plus Kit (GE Healthcare). For dot blots, 1 $\mu$ l of each sample was directly pipetted onto 0.45 $\mu$ m nitrocellulose membrane. After air drying for 20 minutes, the same blocking and detection procedures described above were performed. For total protein staining, SDS-PAGE gels were run as described above and then stained using silver staining (Invitrogen). All images were captured using a Fluor Chem gel documentation system (Alpha Innotech, San Leandro, CA).

**Immunoaffinity purification and gel filtration purification.** For immunoaffinity purification, we utilized the rho1D4 monoclonal antibody (Cell Essentials, Boston, MA) chemically linked to CNBr-activated Sepharose 4B beads (GE Healthcare). The rho-tag1D4 elution peptide **Ac-TETSQVAPA-CONH<sub>2</sub>** was synthesized by CPC Scientific Inc., CA. Rho1D4-Sepharose immunoaffinity purification has been described<sup>16–18</sup>. Gel filtration chromatography was employed for further purification using a HiLoad 16/60 Superdex 200 column on a Äkta Purifier FPLC system (GE Healthcare), as described<sup>16–18</sup>.

**Mass spectroscopy.** Peak fractions from gel filtration were subjected to SDS-PAGE, and stained with Coomassie (SimplyBlue™ SafeStain, Invitrogen). The hTAAR5-T4L gel bands at 47 kDa and 100 kDa were excised into sterile, methanol-rinsed micro-centrifuge tubes. The samples were digested by trypsin, and the resulting fragments were analyzed on Ion Trap LCMS by the MIT Biopolymers Laboratory (Cambridge, MA). Both bands were identified as hTAAR5, indicating monomeric and dimeric forms of hTAAR5-T4L. The hTAAR5 gel band at 33 kDa was identified as hTAAR5.

**Secondary structure analysis using CD spectroscopy.** CD spectra were recorded on a CD spectrometer (Aviv Associates model 410) at 15°C over the wavelength range of 195nm to 260nm with a step size of 1nm and an averaging time of 5 seconds. Spectra for purified hTAAR5 or hTAAR5-T4L monomers were blanked to wash buffer. Spectra were collected with a 111-QS quartz sample cell (Hellma) with a path length of 1mm. The secondary structural content was estimated by using the program K2D2 (<http://www.ogic.ca/projects/k2d2/>). The raw data was first smoothed by using the built-in smoothing function of Aviv software. A manual smoothing was performed using 5-degree sliding polynomial. The CD spectra shown are drawn from the smoothed data.

1. Lindemann, L. *et al.* Trace amine-associated receptors form structurally and functionally distinct subfamilies of novel G protein-coupled receptors. *Genomics* **85**, 372–385 (2005).

- Liberles, S. D. & Buck, L. B. A second class of chemosensory receptors in the olfactory epithelium. *Nature* **442**, 645–650 (2006).
- Fleischer, J., Breer, H. & Strotmann, J. Mammalian olfactory receptors. *Front Cell Neurosci.* **3**, 1–10 (2009).
- Zucchi, R., Chiellini, G., Scanlan, T. S. & Grandy, D. K. Trace amine-associated receptors and their ligands. *Br. J. Pharmacol.* **149**, 967–978 (2006).
- Lindemann, L. & Hoener, M. C. A renaissance in trace amines inspired by a novel GPCR family. *Trends Pharmacol. Sci.* **26**, 274–281 (2005).
- Berry, M. D. The potential of trace amines and their receptors for treating neurological and psychiatric diseases. *Rev. Recent Clin. Trials* **2**, 3–19 (2007).
- Borowsky, B. *et al.* Trace amines: identification of a family of mammalian G protein-coupled receptors. *Proc. Natl. Acad. Sci. U S A* **98**, 8966–8971 (2001).
- Branchek, T. A. & Blackburn, T. P. Trace amine receptors as targets for novel therapeutics: legend, myth and fact. *Curr. Opin. Pharmacol.* **3**, 90–97 (2003).
- Lewin, A. H. Receptors of Mammalian Trace Amines. *AAPS J.* **8**, 138–145 (2006).
- Nelson, D. A., Tolbert, M. D., Singh, S. J. & Bost, K. L. Expression of neuronal trace amine-associated receptor (Taar) mRNAs in leukocytes. *J. Neuroimmunol.* **192**, 21–30 (2007).
- Zeng, Z. *et al.* Cloning of a putative human neurotransmitter receptor expressed in skeletal muscle and brain. *Biochem. Biophys. Res. Communications* **242**, 575–578 (1998).
- Gaillard, I., Rouquier, S. & Giorgi, D. Olfactory receptors. *Cell Mol. Life Sci.* **61**, 456–469 (2004).
- Rosenbaum, D. M., Rasmussen, S. G. & Kobilka, B. K. The structure and function of G-protein-coupled receptors. *Nature* **459**, 356–363 (2009).
- Walian, P., Cross, T. A. & Jap, B. K. Structural genomics of membrane proteins. *Genome Biol.* **5**, 215 (2004).
- Lundstrom, K. Structural biology of G protein-coupled receptors. *Bioorg. Med. Chem. Lett.* **15**, 3654–3657 (2005).
- Reeves, P. J., Kim, J. M. & Khorana, H. G. Structure and function in rhodopsin: a tetracycline-inducible system in stable mammalian cell lines for high-level expression of opsin mutants. *Proc. Natl. Acad. Sci. U S A* **99**, 13413–13418 (2002).
- Cook, B. L., Ernberg, K. E., Chung, H. & Zhang, S. Study of a synthetic human olfactory receptor 17–4: expression and purification from an inducible mammalian cell line. *PLoS One* **3**, e2920 (2008).
- Cook, B. L. *et al.* Large-scale production and study of a synthetic G protein-coupled receptor: human olfactory receptor 17–4. *Proc. Natl. Acad. Sci. U S A* **106**, 11925–11930 (2009).
- Cherezov, V. *et al.* High-resolution crystal structure of an engineered human  $\beta$ 2-adrenergic G protein-coupled receptor. *Science* **318**, 1258–1265 (2007).
- Rosenbaum, D. M. *et al.* GPCR engineering yields high-resolution structural insights into  $\beta$ 2-adrenergic receptor function. *Science* **318**, 1266–1273 (2007).
- Ren, H. *et al.* High-level production, solubilization and purification of synthetic human GPCR chemokine receptors CCR5, CCR3, CXCR4 and CX3CR1. *PLoS One* **4**, e4509 (2009).
- Matthews, B. W. & Remington, S. J. The three dimensional structure of the lysozyme from bacteriophage T4. *Proc. Natl. Acad. Sci. U S A* **71**, 4178–4182 (1974).
- Drew, D., Lerch, M., Kunji, E., Slotboom, D. J. & de Gier, J. W. Optimization of membrane protein overexpression and purification using GFP fusions. *Nat. Methods* **3**, 303–313 (2006).
- Gat, U., Nekrasova, E., Lancet, D. & Natchin, M. Olfactory receptor proteins. Expression, characterization and partial purification. *Eur. J. Biochem.* **225**, 1157–1168 (1994).
- Nekrasova, E., Sosinskaya, A., Natchin, M., Lancet, D. & Gat, U. Overexpression, solubilization and purification of rat and human olfactory receptors. *Eur. J. Biochem.* **238**, 28–37 (1996).
- Katada, S., Nakagawa, T., Kataoka, H. & Touhara, K. Odorant response assays for a heterologously expressed olfactory receptor. *Biochem. Biophys. Res. Commun.* **305**, 964–969 (2003).
- Gurevich, V. V. & Gurevich, E. V. How and why do GPCRs dimerize? *Trends Pharmacol. Sci.* **29**, 234–240 (2008).
- Sarramegna, V., Talmont, F., Demange, P. & Milon, A. Heterologous expression of G-protein-coupled receptors: comparison of expression systems from the standpoint of large-scale production and purification. *Cell Mol. Life Sci.* **60**, 1529–1546 (2003).
- Sarramegna, V., Muller, I., Milon, A. & Talmont, F. Recombinant G protein-coupled receptors from expression to renaturation: a challenge towards structure. *Cell Mol. Life Sci.* **63**, 1149–1164 (2006).

## Acknowledgements

This work is supported in part from **Defense Advanced Research Program Agency-HR0011-09-C-0012**. XW is also supported from a fellowship from China University of Petroleum (East China).

## Author contributions

XW and SZ designed the experiments. XW, KC and CR carried out the experiments. XW analyzed the data. XW, KC and SZ wrote the paper.



## Additional information

**Supplementary information** accompanies this paper at <http://www.nature.com/scientificreports>

**Competing financial interests** The authors declare no competing financial interests.

**License:** This work is licensed under a Creative Commons

Attribution-NonCommercial-ShareAlike 3.0 Unported License. To view a copy of this license, visit <http://creativecommons.org/licenses/by-nc-sa/3.0/>

**How to cite this article:** Wang, X., Corin, K., Rich, C. & Zhang, S. Study of two G-protein coupled receptor variants of human trace amine-associated receptor 5. *Sci. Rep.* 1, 102; DOI:10.1038/srep00102 (2011).